

Gas-phase and aerosol chemistry interactions in South Europe and the Mediterranean region

Marina Astitha · George Kallos

Received: 28 February 2008 / Accepted: 9 October 2008
© Springer Science+Business Media B.V. 2008

Abstract The atmospheric chemical composition is affected by the interaction mechanisms among gases and particulate matter through a wide range of chemical reactions that can occur with the aid of particulate matter (e.g. particles act as reacting or absorbing surfaces) or be influenced by the presence of particulate matter in the atmosphere (photochemical reactions). Physical and chemical processes are also bonded in an interactive way that often leads to the influence of the radiation budget, cloud physics and the warming or cooling of the lower atmospheric levels. The Euro-Mediterranean region is a key-sensitive area due to the unique climatic and air quality characteristics associated with the regional climatic patterns, geomorphology (land and water contrast) and coexistence of pollutants from different origin. Focusing on this region, the gas-aerosol interactions are studied using state-of-the-art atmospheric and chemical transport modeling tools following the necessary development in the chemical transport model CAMx. Sensitivity and large-scale simulations have shown significant responses of the modeling system to the inclusion of natural species emissions, the direct shading effect of dust particles on photochemical processes and the formation of new types of aerosols through heterogeneous uptake of gases on dust particles. Including such interactions in the chemical transport model often led to the improvement of the model performance compared with available measurements in the region.

Keywords Gases · Aerosols · Air pollution · Interaction · Mediterranean · Air quality modeling · Heterogeneous reactions · Dust · Sulfates · Ozone

M. Astitha · G. Kallos (✉)
University of Athens, School of Physics, Division of Environment and Meteorology, Atmospheric Modeling and Weather Forecasting Group, University Campus, Bldg. PHYS-V, Athens 15784, Greece
e-mail: kallos@mg.uoa.gr

M. Astitha
e-mail: marina@mg.uoa.gr

1 Introduction

The interactions between gases and aerosols and their impacts on atmospheric processes and climate have been studied extensively during the past. The scientific basis of these interactions is rather wide, requiring the expertise and collaboration of major scientific fields to reach into some vital conclusions. Results from such collaboration have been stated recently from the 4th IPCC Assessment Report [1] in which, observations, modeling and analysis techniques have led to conclusions on the climate change aspects.

Euro-Mediterranean is a region sensitive to interactions between gas-phase and aerosol chemical processes due to the coexistence of anthropogenic and natural atmospheric pollutants and the morphology of the area [2–14]. In several occasions, such coexistence can create air quality conditions that exceed the imposed air quality guidelines [15]. The physico-chemical processes allowing the interactions between gas-phase and aerosol constituents will be the primary focus of the work presented herein. For that purpose, atmospheric pollutants have been categorized as first generation (primary, such as sulfur dioxide, nitrogen oxides, desert dust and sea salt, among others), second generation (secondary, like ozone, sulfates and nitrates) and third generation pollutants which are formed through reaction paths between the previous categories [14].

The processes linking the above generations of pollutants require extensive investigation since they are complex and uncertain and model development is essential to include the relevant physicochemical processes [16]. The interactions have been studied using atmospheric and air-quality modeling tools following the necessary development in a state-of-the-art chemical transport model. In particular, the new development has included the impacts of desert dust on photochemical processes, the sea salt particle production and the treatment of soil dust particles as reactive agents (through the incorporation of heterogeneous chemical processes).

In the next section, the gas-aerosol interactions dealt by this study are outlined. In the third section follows the brief description of the modeling systems and the model configurations for the performed simulations. The fourth section comprises of the model sensitivity studies on each of the interactions described, beginning with the shading effect of dust on photochemical production, the sea salt production and finally the new particle formation based on heterogeneous reactions on dust particles. The capabilities of the new model development and the first results obtained so far are the subject of discussion in the final section together with the derived conclusions.

2 Interactions between gases and aerosols

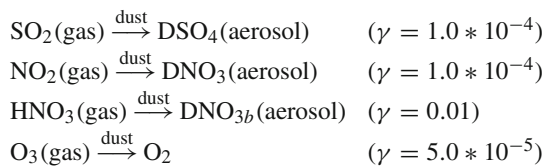
The earth's atmosphere consists of gases and particulate matter, bonded in a dynamic system that changes its composition depending on the exchanges between atmosphere, ocean and land. These constituents are emitted directly in the atmosphere or formed during chemical reactions that occur at several altitudes or near the surface. A great number of physical and chemical processes are responsible for the alteration of the atmospheric composition, such as anthropogenic and natural emissions and the interactions among the emitted constituents.

The Euro-Mediterranean region is sensitive to naturally emitted species like sea salt and desert dust, among others. On the other hand, man-emitted species have their main sources in the European continent and in several Eastern European countries that do not adhere to legislative measures. Consequently, the interactions between gases and aerosols are important for the region, mostly because the results from these interactions can cause several effects

on air quality and the physical environment. Increased particulate matter concentrations can produce levels of pollutants high above the EU limit values, affecting the air quality. Influences on the radiation budget, cloud formation, precipitation efficiency and the heating or cooling of the atmosphere [17–19], affect the physical environment. Overall, from an air quality perspective, the feedbacks between atmospheric pollutants and the physical environment are interesting and worth extensive investigation.

For the definition of the interactions, the first step has been the acknowledgement of the direct shading effect that dust particles have on photochemical processes [13]. In that way, the presence of dust aerosols in the atmosphere influence gases like ozone. The second interaction is delineated through the direct emissions of sea salt particles from the sea surface and/or the surf zone [20]. Sea salt particles are speciated into sodium, chloride and sulfate particles, transported away from their origin and interacting with other species in the atmosphere [14, 21, 22]. The third interaction is realized through heterogeneous chemistry pathways, especially the heterogeneous formation of new aerosols on the surface of desert dust particles [14, 15, 18].

The interactions described above are implemented in the chemical transport model CAMx [23] enabling the possibility to study the impacts of such interactions in the Euro-Mediterranean atmosphere. The implementation procedure comprises of the following steps: implementation of dust optical depth in the calculation of photolysis rates during severe dust transport episodes [13], development of sea salt production directly inside the air quality model [20] and heterogeneous uptake of gases on dust particles [14]. The production of sea salt has been based on the work of Gong [22], Zhang et al. [24] for the open ocean function and the work of de Leeuw et al. [25] and Gong et al. [26] for the surf zone function. The heterogeneous reactions on dust particles follow the formulation of Fuchs and Sutugin [27], Saylor [28] and Dentener et al. [29]. The implemented reactions and the uptake coefficients for each reaction are:



Uptake coefficients (γ -values) for each heterogeneous reaction have been selected based on published work for experimental and modeling studies, trying to assign the most appropriate values for Saharan dust particles. Table 1 presents the uptake coefficients for each of the above reactions based on several publications. The values denoted with bold fonts are the ones chosen for the performed simulations. A brief description of the modeling systems used for this study is the subject of the following section, including the analytical representation of the model configuration for the simulations performed with the chemical transport model.

3 Model description

A short description of the modeling systems used for performing simulations is provided in this section: *The SKIRON/Dust* is a modeling system developed at the University of Athens from the Atmospheric Modeling and Weather Forecasting Group [4, 48, 49]. It incorporates several state-of-the-art parameterizations for the description of the production, transport and removal processes of the desert dust cycle. The soil moisture and turbulent state of the atmosphere play a critical role for dust uplift and injection into the air. Since the dust cycle module

Table 1 Uptake coefficients (γ -values) of gases on dust particles based on published work

| Reference | γ_{SO_2} | γ_{NO_2} | γ_{HNO_3} | γ_{O_3} | Method |
|---------------------------|--|--|--------------------------------|---|------------------------|
| Seisel et al. [30] | $(7.6 \pm 0.5) \times 10^{-2}$ | | | | Laboratory |
| Chang et al. [31] | | | | 2×10^{-7} – 6×10^{-6} | Laboratory |
| Adams et al. [32] | $(6.6 \pm 0.8) \times 10^{-5}$ | | | | Laboratory |
| Seisel et al. [33] | | | $(5.4 \pm 0.5) \times 10^{-2}$ | | Laboratory |
| Ullerstam et al. [34] | $(5.7 \pm 1.9) \times 10^{-6}$ | | | | Laboratory |
| Hanisch and Crowley [35] | | | 0.1 | 7×10^{-6} – -3×10^{-5} | Laboratory |
| Usher et al. [36] | $(1.6 \pm 0.5) \times 10^{-4}$ | | | | Laboratory |
| Ullerstam et al. [37] | | $(2.0 \pm 0.4) \times 10^{-4}$ (geom.surface) $(6.3 \pm 1.0) \times 10^{-7}$ (BET surface) | | 10^{-2} – 10^{-4} (geom.surf) 10^{-6} – 10^{-8} (BET surf) | Laboratory |
| Hanisch and Crowley [38] | | | $(11 \pm 3) \times 10^{-2}$ | | Laboratory |
| Underwood et al. [39] | | 10^{-4} | $(2.0 \pm 0.1) \times 10^{-5}$ | | Laboratory |
| Goodman et al. [40] | 10^{-4} | | | | Laboratory |
| Bauer and Koch [41] | 10^{-4} | | | | Simulation, field exp. |
| Tang et al. [42] | 10^{-4} | 10^{-4} | 0.01 | 5×10^{-5} | Simulation |
| Liao et al. [43] | 3×10^{-4} (RH < 50%) 0.1 (RH > 50%) | 10^{-4} | 0.1 | 5×10^{-5} | Simulation |
| Bauer et al. [44] | | | 0.1 | 10^{-5} | Simulation, field exp. |
| Liao et al. [45] | 3×10^{-4} (RH < 50%) 0.1 (RH > 50%) | 10^{-4} | 0.1 | 5×10^{-5} | Simulation |
| Bian and Zender [46] | | 4.4×10^{-5} | 1.1×10^{-3} | 5×10^{-5} | Simulation |
| Zhang and Carmichael [47] | 10^{-4} | | 0.01 | 10^{-4} | Simulation |
| Dentener et al. [29] | 3×10^{-4} (RH < 50%) 0.1 (RH > 50%) | | 0.1 | 5×10^{-5} | Simulation |

is dynamically coupled to the atmospheric model, the prognostic atmospheric and hydrological conditions are used to calculate the effective rates of the injected dust at each time step. The version of the model used for this study, has four particle size bins with centered diameters at 1.5, 12, 36, and 76 μm [50]. The ability of the model to predict the dust concentration has been validated with available measurements in several studies [4, 5].

The *Comprehensive Air Quality Model with Extensions (CAMx)* [23] is an Eulerian photochemical model that allows for integrated assessment of air-pollution over many scales ranging from urban to super-regional (<http://www.camx.com>). CAMx has also model structures for modeling aerosols, processes that are linked to the CB4 gas phase chemical

mechanism, science modules for aqueous chemistry (RADM-AQ) inorganic aerosol thermodynamics/partitioning (ISORROPIA, [51]) and secondary organic aerosol formation/partitioning (SOAP).

The atmospheric modeling system SKIRON/Dust is coupled offline with the chemical transport model CAMx. Meteorological and dust-related fields produced from SKIRON, feed CAMx model to drive the air quality simulations. Improvement of the coupling between the two models consists of the development of sub-systems handling processes that are not included in the chemical transport model. Specifically, calculated desert dust optical depth in the preprocessing stage of the air quality simulations is used to influence the rates of photolytic reactions in the presence of desert dust. Also, surface fluxes of desert dust enrich the emissions preprocessor providing the capability of simulating particles originated from soil in different size sections within the CAMx model (CAMx model identifies desert dust as crustal material, [23]). More details related to the techniques and methodologies adopted are provided in Sect. 4.1.

During each stage of the development/improvement of the chemical transport model, sensitivity and long-run simulations took place. The sensitivity tests relate to the shading effect of dust particles on photochemical processes. The long-run simulations incorporate all of the gas-aerosol interaction processes described in the previous section. Tables 2 and 3 summarize the configuration of the modeling systems, for each type of simulation performed. Constant in space and time boundary conditions (concentrations of the relevant species) are imposed in all of the performed simulations. The species involved are NO, NO₂, O₃, NMVOC, CO, HONO, HNO₃, SO₂, NH₃, PSO₄, PNO₃, N₂O₅, isoprene etc. The values chosen for the boundary conditions are based on climatological data and the area covered is large enough to reduce the boundary effects.

In the simulations (meteorological and air quality) the domains are focused on the Mediterranean region with some differences in the extension of the area covered, depending on the type of simulation. In brief, SKIRON/Dust modeling system domain covers the Mediterranean region, Europe and the largest part of the African continent. The domain used for

Table 2 Model configuration for the sensitivity simulations

| | |
|-----------------------------|--|
| SKIRON/Dust modeling system | |
| Input data | ECMWF initial and lateral boundary conditions ($0.5^\circ \times 0.5^\circ$) on 11 isobaric levels; topography ($30'' \times 30''$): US Geological Survey (USGS) dataset; vegetation ($30'' \times 30''$): USGS dataset; Soil ($2'' \times 2''$)—ZOBLER and FAO/UNESCO |
| Horizontal resolution | $0.24^\circ \times 0.24^\circ$ |
| No of grid points | 135×213 |
| No of vertical layers | 38 (up to 22 km) |
| Simulation period | 15–18 April 2005 22–25 February 2006 |
| CAMx | |
| Input meteorological data | 3D meteorological fields from SKIRON/Dust |
| Input air quality data | Gridded initial and boundary conditions, time/space constant concentrations |
| Input emission data | Gridded area sources from EMEP database ($16 \times 16 \text{ km}^2$; Hertel et al. [65]) |
| Horizontal resolution | $0.235^\circ \times 0.18^\circ$ |
| No of grid points | 200×108 |
| SW corner of the grid | ($-7^\circ, 28^\circ$) |
| No of vertical layers | 14 (up to 4 km) |
| Chemical mechanism | CB-IV with full aerosol chemistry (ISORROPIA, SOAP, RADM), CF approach (coarse/fine) |
| Simulation period | 15–18 April 2005 22–25 February 2006 |

Table 3 Model configuration for the large-scale simulations

| | | |
|-----------------------------|--|--------------------------------|
| SKIRON/Dust modeling system | | |
| Input data | ECMWF initial and lateral boundary conditions ($0.5^\circ \times 0.5^\circ$) on 16 isobaric levels; topography ($30'' \times 30''$); US Geological Survey (USGS) dataset; vegetation ($30'' \times 30''$); USGS dataset; Soil texture ($1'' \times 1''$)—ZOBLER and FAO/UNESCO | |
| Horizontal resolution | $0.24^\circ \times 0.24^\circ$ | $0.16^\circ \times 0.16^\circ$ |
| No of grid points | 135×213 | 245×315 |
| No of vertical layers | 38 (up to 22 km) | |
| Simulation period | 28 July–22 August 2001 | 1–20 April 2003 |
| CAMx | | |
| Input meteorological data | 3D meteorological fields from SKIRON/Dust | |
| Input air quality data | Gridded initial and boundary conditions, time/space constant concentrations | |
| Input emission data | Gridded area sources from EMEP database ($16 \times 16 \text{ km}^2$; Hertel et al. [65]) Gridded area sources from GEIA ($1^\circ \times 1^\circ$) (www.geiacenter.org) | |
| Horizontal resolution | $0.235^\circ \times 0.18^\circ$ | |
| No of grid points | 200×108 | 305×231 |
| SW corner of the grid | $(-7^\circ, 28^\circ)$ | $(-16.5^\circ, 11.5^\circ)$ |
| No of vertical layers | 14 (up to 4 km) | 22 (up to 8 km) |
| Chemical mechanism | CB-IV with full aerosol chemistry (ISORROPIA, SOAP, RADM). CMU approach (3 size bins): 0.03–0.1, 0.1–2.5, 2.5 – 10 μm | |
| Simulation period | 1–22 August 2001 | 1–20 April 2003 |

CAMx simulations differs for the two-types of simulations on the width of the selected area. For the sensitivity simulations and the large-scale simulation for August 2001, the domain covers mostly the Mediterranean region, Central, Eastern and part of Western Europe, as well as part of North Africa. For the case of April 2003, the extended domain includes the desert areas of the African continent (north and central Africa) and large part of the Arabian Peninsula. During April, the transport of desert dust towards the Mediterranean is favored and large quantities of dust particles travel thousand of kilometers from Saharan desert to Eastern and Central Mediterranean region. The horizontal resolution is rather coarse (approximately 20 km) due to the necessity to analyze the pollutant movement in the large area of interest and due to restrictions in the emission inventory spatial resolution.

Synoptic meteorological conditions are of major interest during the process of selecting the simulation periods, always depending on the objectives of the conducted study. In this manuscript, we discuss simulations for three different periods (August 2001, April 2003 and February 2006). In brief, the meteorological conditions differ during the mentioned periods of the year, sharing one common ground: the transport of desert dust from Central and Northern Africa toward Europe. In the present work, the coexistence of pollutants originated from different sources is of major importance in order to study the interactions among them.

During August, the synoptic conditions in the Mediterranean region are driven by strong northerly winds, limited amounts of precipitation and intense photochemical activity.

During April, the formation of low-pressure systems is evident. These systems move eastward relatively fast. Precipitation occurs in several parts of the domain and western, south-western or sometimes southern winds transport large amounts of desert dust from Africa to Europe over the Mediterranean Sea.

February is a month of the year with limited photochemical activity in general, but during the specific days of February 2006, a severe episode of dust transport toward the Eastern Mediterranean occurred. This is an interesting case study for simulating the radiative effects of dust.

In general, desert dust transport occurs on an episodic basis. A summary of the synoptic conditions favoring the long-range transport of natural and anthropogenic pollutants can be found in Kallos et al. [5] and references therein.

4 Model sensitivity studies on the gas-aerosol interactions

4.1 Sensitivity of photolysis rates

The description of the first gas-aerosol interaction focuses on the shading effect of dust particles that cause alterations in the photolysis rates. Primarily, Astitha et al. [13] have presented such interaction for an extreme desert dust episode in the Eastern Mediterranean (for April 2005). A second episode occurred on February 2006, lasted for 3–4 days and affected the visibility and air quality of Greece as shown in Fig. 1. PM₁₀ levels for both episodes have been recorded high above $1,000 \mu\text{g m}^{-3}$ for Athens and Crete Island (sources: Hellenic Ministry for the Environment, Physical Planning and Public Works and Professor N. Mihalopoulos ECPL, Department of Chemistry, Crete).

The episode of February 2006 has been analyzed using SKIRON/Dust and CAMx models (model configuration is presented in Table 1), considering only the effects of dust optical depth on photochemical reactions. Dust optical depth is calculated using the dust load fields from SKIRON and mass extinction coefficients for each particle size and wavelength ($Dust\ Optical\ Depth = Dust\ Load\ (\text{g/m}^2) \times Mass\ Extinction\ Coefficient\ (\text{m}^2/\text{g})$, from Seinfeld and Pandis [52], Tegen et al. [53] and Chin et al. [54]). The appropriate mass extinction coefficient for each particle size at 340 nm wavelength is obtained from Anderson et al. [55] and the database of the Geophysical Fluid Dynamics Laboratory (GFDL) radiation model. For dust particles with centered diameter at $1.5 \mu\text{m}$, the mass extinction coefficient is $0.8912 \text{ m}^2 \text{ g}^{-1}$ and for dust particles with centered diameter at $12 \mu\text{m}$, the mass extinction coefficient is $0.0782 \text{ m}^2 \text{ g}^{-1}$ at 340 nm. The other two larger size sections (36 and $76 \mu\text{m}$) are not included in this study, since they are quite heavy to transport far away from their source. Calculated dust optical depth at 340 nm wavelength is in accordance with the TUV

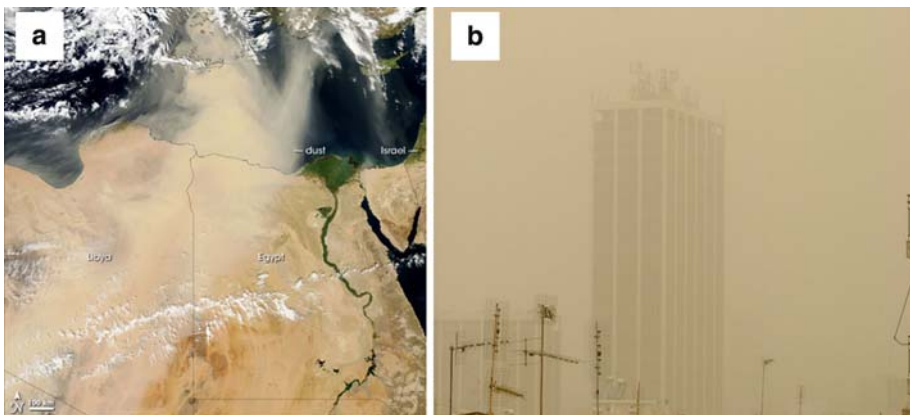


Fig. 1 a Dust transport from Northern Africa toward Eastern Mediterranean from NASA GSFC Satellite (<http://earthobservatory.nasa.gov/>). b Photographic image of Athens centre for February 24, 2006

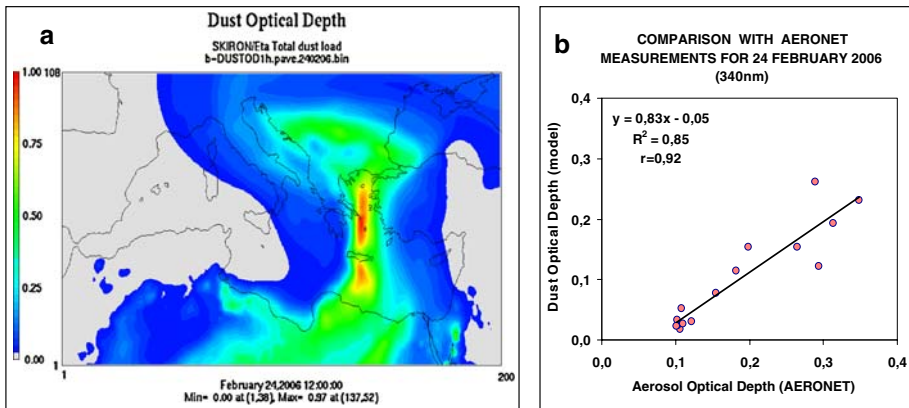


Fig. 2 **a** Dust optical depth calculated by the model at 12:00 UTC, February 24, 2006. **b** Comparison of dust optical depth with measurements at several AERONET sites for the same day

(Tropospheric Ultraviolet-Visible Model, [56]) model, which uses a look-up table for aerosol optical depths for a standard atmosphere at 340 nm.

The dust optical depth calculated from the dust concentrations has reached values higher than 0.9 as shown in Fig. 2a. These values compare well with the available AERONET Aerosol Optical Depth measurements (Fig. 2b). The model-observation comparison for the period of February 2006 gave correlation coefficient (r) 0.92 (Fig. 2b), providing some assurance on the credibility of the applied methodology.

Since the calculation of dust optical depth has shown reasonable results compared to the observations, the next step has been the utilization of dust optical depth in the calculation of photolysis rates. The TUV model (Tropospheric Ultraviolet-Visible Model, [56,57]) calculates the photolysis rates, using the clear-sky assumption. The correction for the presence of clouds occurs during runtime, within CAMx model [58]. The procedure followed for the inclusion of dust optical depth in the calculation of photolysis rates begins with the SKIRON/Dust simulation. The dust-related fields from SKIRON/Dust modeling system are incorporated in a pre-processor to handle the changes in geographical projection and calculate the dust optical depth for specific wavelengths on an hourly basis, as described in the previous paragraph. The standard version of TUV model uses a look-up table for the vertical profile of aerosol optical depth (standard atmosphere) at 340 nm (wavelength) from Elterman [59]. Dust optical depth in combination with that look-up table for each grid cell of the modeling domain, result in the calculation of photolysis rates, which are different from the calculation via the original version of the TUV model.

Photolysis rates for ozone ($J(O_1D)$) have showed a reduction at the surface and up to 1.5–2 km for Athens area, where the dust plume was located. Figure 3a shows the vertical distribution of the ozone photolysis rates with and without the inclusion of the dust influence, focused on Athens area in the model domain, at 12:00UTC. The blue line shows the photolysis rates using the original version of TUV model and the red line the rates after implementing the radiative effects of dust in the TUV model. Figure 3b presents the vertical distribution of dust concentration above Athens area for the same period and reveals the stratification of the dust plume in the lower atmosphere. The dust plume extends to 1.5 km above the surface and that explains the small increase in photolysis rates above the plume in Fig. 3a, probably because of scattering effects on the dust particles.

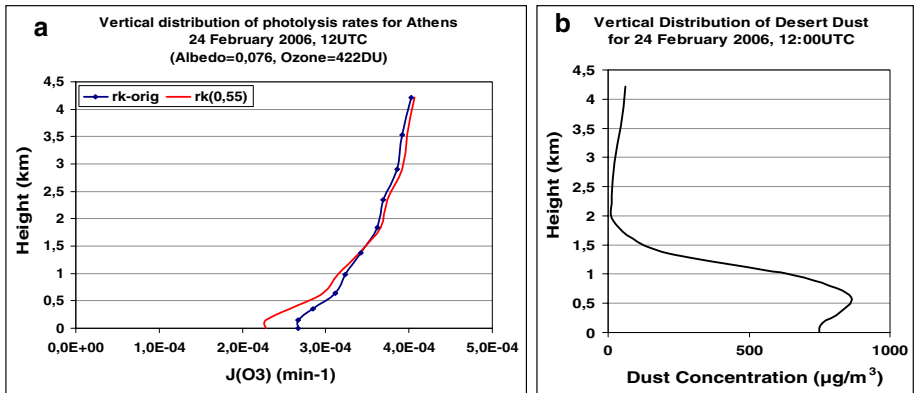


Fig. 3 **a** Vertical distribution of ozone photolysis rates for Athens area during February 24, 2006, at 12UTC, calculated by the model. The blue line denotes the photolysis rates without the dust influence and the red line the altered rates with the inclusion of dust. **b** Vertical distribution of total dust concentration calculated by SKIRON/Dust model for Athens area during February 24, 2006, at 12UTC

On the 24th of February, during noon time above Athens, the dust optical depth was approximately 0.55 and the dust concentration reached $750 \mu\text{g m}^{-3}$. This resulted in a decrease in NO_2 and O_3 photolysis rates, approximately 14.8% and 14.5% at the surface (the decrease is calculated as $(J_{\text{dust}} - J_{\text{normal}})/J_{\text{normal}} * 100\%$). In areas where dust optical depth was 0.7–0.8 the photolysis rates decrease reached 20% for both reactions. $J(\text{O}1\text{D})$ at the surface above Athens was $0.0003 \text{ min}^{-1} = 0.5 * 10^{-5} \text{ s}^{-1}$ (Fig. 3a) and $J(\text{NO}_2)$ was $0.3 \text{ min}^{-1} = 0.005 \text{ s}^{-1}$ for February at noon time. Both values are in agreement with the measurements of Balis et al. [60] and Gerasopoulos et al. [61] for Crete Island.

In general, the sensitivity tests conducted for the influence of desert dust on photochemical reactions, showed reduction of photolysis rates at the surface, reaching 20% in severe Saharan dust episodes (dust concentration $1,100 \mu\text{g m}^{-3}$). In Martin et al. [62], the model results showed 5–20% reduction of the photolysis rates for NO_2 and O_3 during August, over most of the Northern Hemisphere, which agrees with the results from our simulations. After performing two simulations with the chemical transport model CAMx, the outcome was the estimated differences in ozone and sulfate concentrations. The first simulation, called ‘normal’ has utilized the photolysis rates from the original version of the TUV model, whereas in the second simulation called ‘dust’, the altered photolysis rates due to the presence of dust particles are used. The simulations performed with and without the radiative effects of dust on photochemical reactions, showed a maximum reduction in ozone and fine sulfate concentration of the order of 1–2 ppb and $1\text{--}2 \mu\text{g m}^{-3}$, respectively, at the surface and at higher atmospheric layers. The maximum reduction in ozone concentration was approximately 2–3% of the base-case concentration, a result that agrees with the work of Tang et al. [42] during the ACE-ASIA experiment. Figure 4 illustrates the discussed reductions for ozone and fine particulate sulfate at the first layer of the model, for February 24, 2006 at 12:00UTC.

The attenuation of the photolysis rates due to clouds is a very crucial factor that drives the photolytic loss or production of atmospheric species. In the simulations described herein, cloud effects are accounted for during runtime, correcting the photolytic reactions with and without the inclusion of desert dust shading effect. The net reduction in ozone and sulfate concentration discussed in this section is a result solely from the inclusion of dust in the calculation of the j -values. A small increase in the base-case value appeared in ozone and

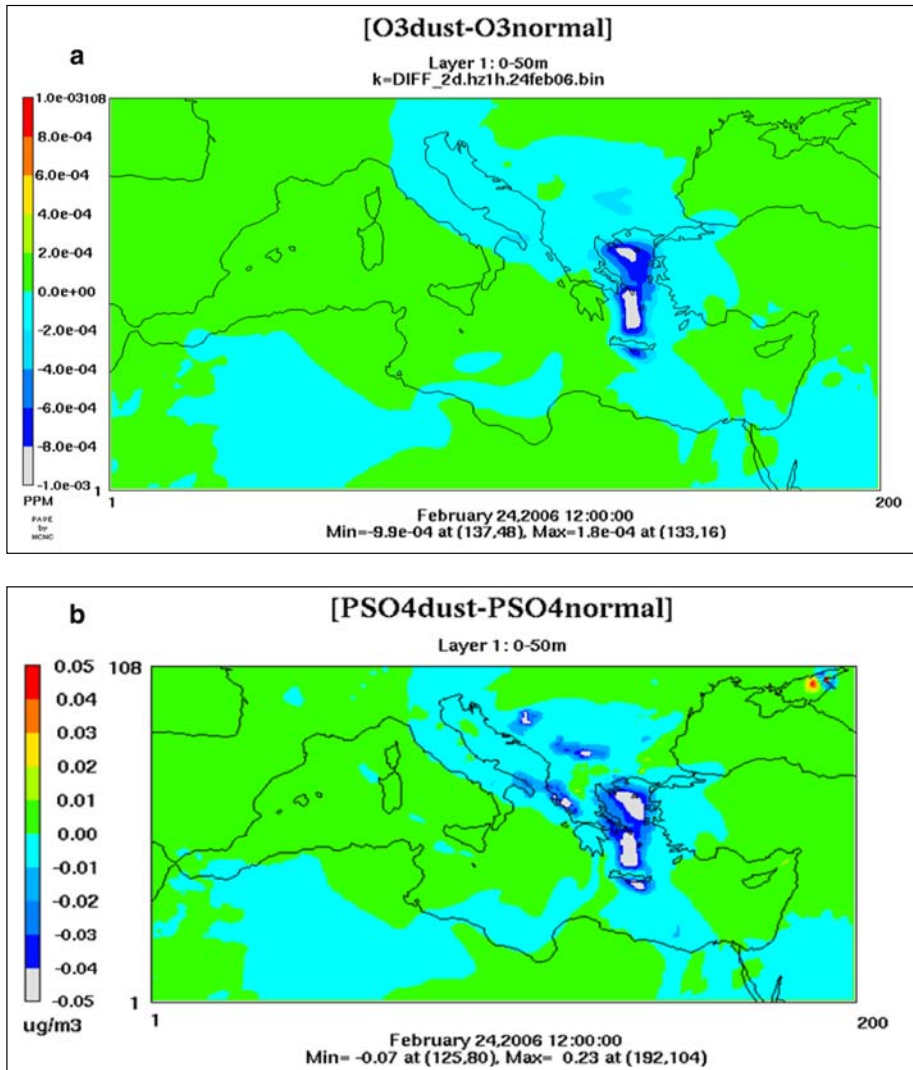


Fig. 4 Hourly changes in (a) ozone and (b) fine particulate sulfate for February 24, 2006, at 12:00UTC. The difference is between a simulation with the inclusion of dust optical depth (called dust) and a simulation without dust (called normal)

sulfate concentrations at the first model layer, for specific locations in the domain, instead of the expected decrease (Fig. 4). This can be attributed to low photolytic losses below the dust plume that can produce accumulation of the photochemical species formed during the previous day. For fine sulfate, the increase is of the order of $0.04\text{--}0.2\ \mu\text{g}/\text{m}^3$ and spans an area of approximately 20 grid cells (total area of $4.7^\circ \times 3.6^\circ$). Another reason additive to the transport from the previous day relates to the aerosol optical depth. The main difference between the base-case simulation and the one with the inclusion of dust is the calculation of the photolysis rates. Predictive aerosol optical depth is used instead of the constant value of “haze” (0.094 in CAMx version 4.03 and 0.1 in later versions) in the base-case simulation.

Consequently, there are parts of the simulation domain where the calculated photolysis rates are using lower values for optical depth than the default value (base-case simulation). Overall, the impact of Saharan dust on the photochemical production of ozone and particulate sulfate can be described as minor but not negligible for areas like the Euro-Mediterranean region characterized by high photochemical activity.

4.2 Sensitivity of sea salt production

Sea salt particle production has been the second step toward the study of the interactions between gases and aerosols of natural and anthropogenic origin. The purpose of including the sea-salt production module in the chemical transport model was the strengthening of the physical and chemical processes with naturally originated species. Sea-salt aerosols interact with gases on an indirect way, enriching the chemical processes with sodium, chloride and sea-salt sulfate that consequently influence the production/destruction of several other species. Sea-salt is not treated as a reactive surface in the current version of the model.

Large-scale simulations (described in Sect. 3) have been performed with the inclusion of sea-salt production (sea-salt is speciated into sodium, chloride and sulfate aerosol using the factors $f_{\text{Na}} = 0.3856$, $f_{\text{Cl}} = 0.5389$, $f_{\text{SO}_4} = 0.0755$, respectively), as suggested by Shankar et al. [20] and Gong [22]. Available measurements of sodium aerosol concentration in the Euro-Mediterranean region assist in the evaluation process. The statistical analysis performed for the modeled versus observed coarse sodium aerosol concentration (PM10) is summarized in Table 4. The analysis showed a reasonable linear correlation with correlation coefficients ranging from 0.67 to 0.76. The biases and root mean square errors are rather acceptable, revealing the model over/underestimation depending on the seasonality, frequency sampling and location of the station.

As expected from the theoretical formulation of sea-salt production, the sodium and chloride aerosols generated from the model experienced peak concentrations in cases with high surface wind and relative humidity. Surface wind speed of the order of $15\text{--}20\text{ m s}^{-1}$ gave hourly concentrations of aerosol chloride and sodium that reached 70 and $60\text{ }\mu\text{g m}^{-3}$,

Table 4 Statistical analysis of modeled versus observed sodium aerosol concentrations

| | Finokalia station, Crete | | Spain | |
|---------------------------------|--|----------------------------------|--------------------------------------|----------------------------------|
| | Model ($\mu\text{g}/\text{m}^3$) | Obs ($\mu\text{g}/\text{m}^3$) | Model ($\mu\text{g}/\text{m}^3$) | Obs ($\mu\text{g}/\text{m}^3$) |
| 1–22 August 2001 | | | | |
| 3 h average Na (bulk) | 2.34 ± 1.43 | 1.69 ± 1.14 | | |
| Daily average Na (PM10) | | | 0.95 ± 0.8 | 1.29 ± 0.6 |
| Linear correlation (trend line) | $y = 0.873 \times +0.904$ $r = 0.67$ | | $y = 0.94 \times -0.27$ $r = 0.7$ | |
| Bias | 0.61 | | -0.34 | |
| RMSE | 1.31 | | 0.67 | |
| 1–18 April 2003 | | | | |
| | Finokalia station, Crete | | Obs ($\mu\text{g}/\text{m}^3$) | |
| Daily average Na (PM10) | Model ($\mu\text{g}/\text{m}^3$) | | 1.73 ± 0.76 | |
| Linear correlation (trend line) | 1.17 ± 0.83 $y = 0.838 \times -0.283$ $r = 0.76$ | | | |
| Bias | -0.56 | | | |
| RMSE | 0.75 | | | |

Table 5 Modeled PM10 sodium aerosol concentration for specific grid cells

| PM10 Sodium aerosol concentration ($\mu\text{g}/\text{m}^3$) | Hourly maximum value | Daily maximum value | Average in the simulation period |
|--|----------------------|---------------------|----------------------------------|
| 1–22 August 2001 | 21.7 | 15.72 | 2.59 |
| 1–20 April 2003 | 61.5 | 18.4 | 3.02 |

respectively. In an attempt to justify the high amounts of sodium aerosol within the first model layer (0–50 m), we gathered information from publications related to sea-salt.

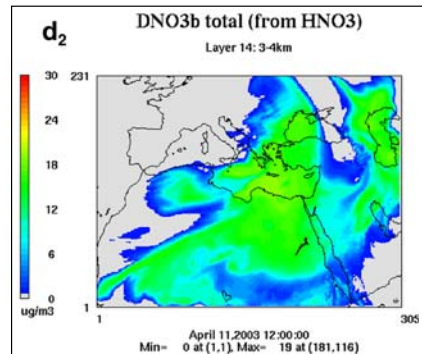
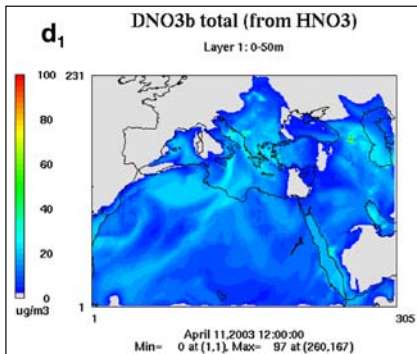
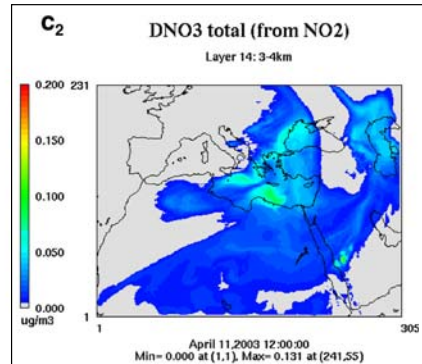
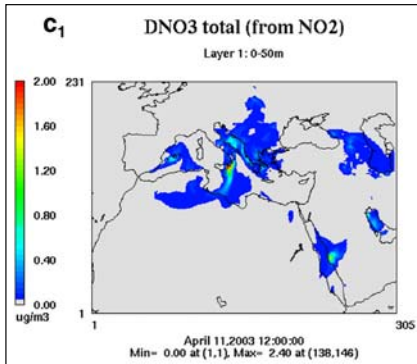
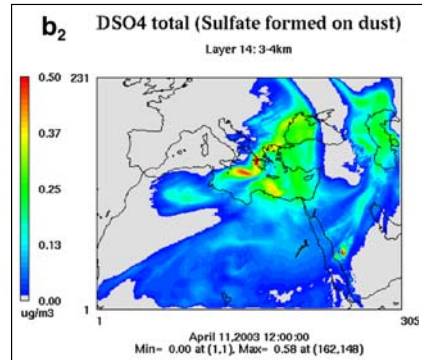
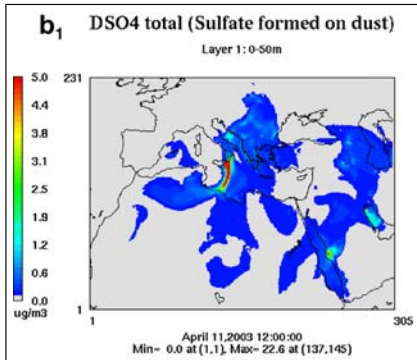
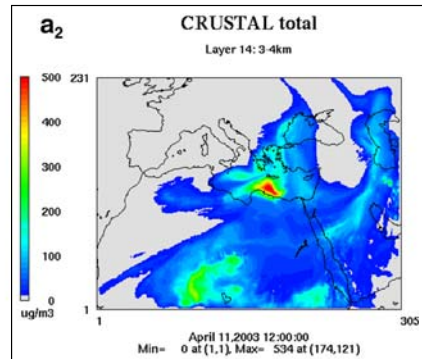
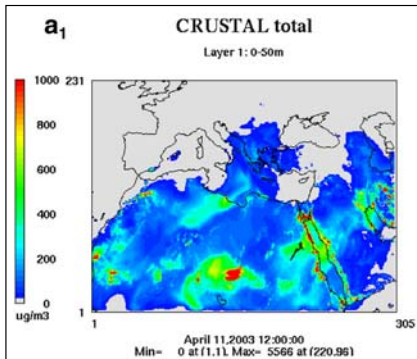
Monthly averages of bulk sodium aerosol obtained from Gong et al. [26] in the Atlantic Ocean were 20, 8 and $4 \mu\text{g m}^{-3}$ for February, April and August, respectively. Measurements in Crete Island [63] gave a summer average sodium aerosol concentration of $2.027 \mu\text{g m}^{-3}$. Finally, Alastuey et al. [15] measured sodium aerosol concentration (Total Suspended Particles-TSP) of the order of $20 \mu\text{g m}^{-3}$ at the Canary Islands (three-day average). For the case of August 2001, the selected modeled point is in the Central Mediterranean, while for the case of April 2003, the selected point is in the Western Mediterranean. Each of the simulation periods covers practically 1 month in length. The calculated average is referred to as a mean monthly value as illustrated in the last column of Table 5. The modeled quantities shown in Table 5 compare with the ones from the referred publications on an acceptable way. Nevertheless, the uncertainties attributed to various factors such as the representation of the meteorology, salinity and coastline complexity are still high.

4.3 Sensitivity of new particle formation

The final step in studying the interactions between gas-aerosol chemistry has been the inclusion of the previous processes along with the heterogeneous reactions of gases on dust particle surface. Thus, the coexistence and interaction of pollutants from different origins (natural and anthropogenic) can be fully handled by the chemical transport model. The large-scale simulations discussed in Sect. 3 have been performed with all the new processes included, using meteorological fields from SKIRON/Dust modeling system. CAMx multi-sectional approach has been implemented for the treatment of particulate matter, with three size sections, each having diameters in ranges: 0.03–0.1, 0.1–2.5, 2.5–10.0 μm . CAMx model runs on a latitude–longitude projection, with horizontal resolution $0.235^\circ \times 0.18^\circ$ (Table 3). Results for the April 2003 simulation are discussed in this section, since April is the month of significant dust transport towards the Mediterranean region and efficient photochemical activity. Figure 5 displays the concentrations of the new aerosols formed on dust particles for two model layers, near the surface (0–50 m) and in the upper troposphere (3–4 km), for April 11, 2003, a day with significant transport of dust to the Eastern Mediterranean Region.

In general, the amount of sulfate produced on dust (DSO4) is rather small, about $2\text{--}4 \mu\text{g m}^{-3}$ (in 2 h average), except in areas with fresh and continuous sulfur dioxide emissions in conjunction with the availability of dust in the area, like southern Italy and Saudi Arabia (Fig. 5b₁ and b₂). The 2 h-average values of DSO4 are in accordance with Zhang and

Fig. 5 2 h average total concentration in two vertical layers, 0–50 m (left graphs) and 3–4 km (right graphs) ► for: (a) crustal material (Saharan dust), (b) sulfate produced on dust (DSO4), (c) nitrate produced on dust via NO_2 reaction (DNO3), (d) nitrate produced on dust via HNO_3 reaction (DNO3b), for April 11, 2003, at 12:00UTC



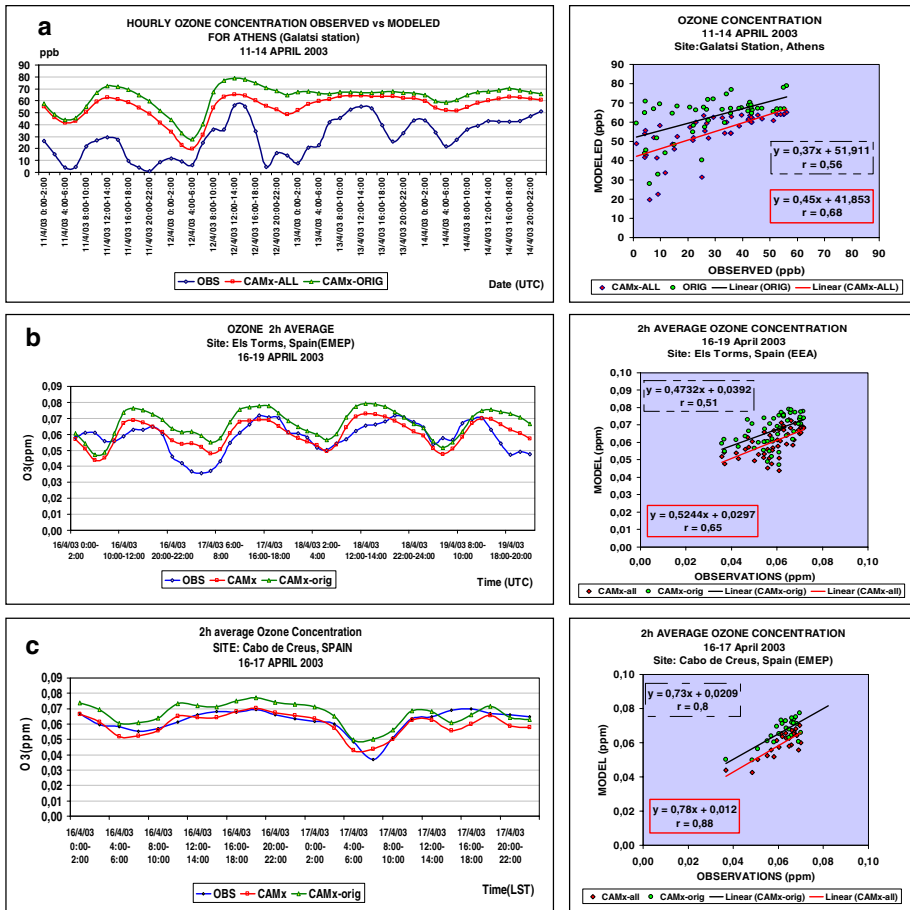


Fig. 6 Time series and linear-correlation of ozone concentration at the first model layer with observations at three sites: (a) Station in Athens basin (Galatsi-urban background) for 11–14 April 2003, (b) EMEP station in Spain (Els Torms-rural background) for 16–19 April 2003 and (c) EMEP station in Spain (Cabo de Creus-rural background) for 16–17 April 2003. The green lines on the left plots and green dots on the right scatter diagrams are associated with the original model simulation. Red lines on the left and red dots on the scatter diagrams are associated with the new-processes model development

Carmichael [47]. The overall contribution of DSO4 to the total sulfate concentration can be characterize as minor, except in cases with fresh and continuous sulfur emissions and dust transport (as discussed previously) where the DSO4 can alter the general trend of sulfates in the area. Nitrate produced on dust from the nitrogen dioxide reaction is rather small, with values lower than the DSO4 produced (Fig. 5c₁ and c₂) for both atmospheric layers. Nitrate produced on dust from the nitric acid reaction exhibits larger concentration values, reaching 20–40 μg m⁻³ (2h average) (Fig. 5d₁ and d₂).

The major uncertainties in these simulations relate to the uptake coefficient (gamma value-γ) used for the calculation of the heterogeneous uptake of gases on dust surface. Overall, the model simulated total sulfate (as sum of anthropogenic and formed on dust) in a reliable way, coinciding with various publications on this field [41,43,45,47]. The comparison with observations showed correlation coefficients that varied from 0.5 to 0.8 depending on the

location, with the model slightly over-predicting the observations (modeled values were 1 to 1.5 times the measured ones). The results were also satisfactory for the nitrate formed on dust based on the published data, but because CAMx has a tendency to over-predict nitrates in its original code [64], the comparison with observations revealed such over prediction once more.

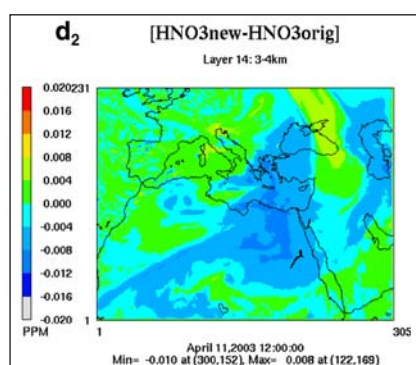
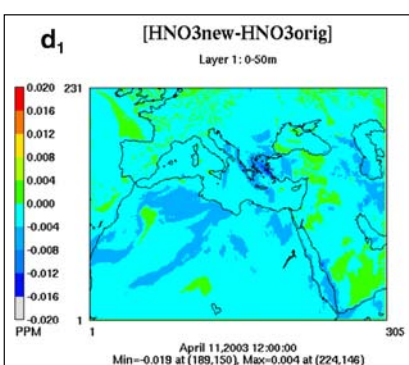
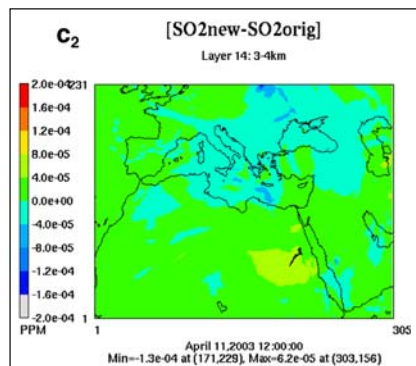
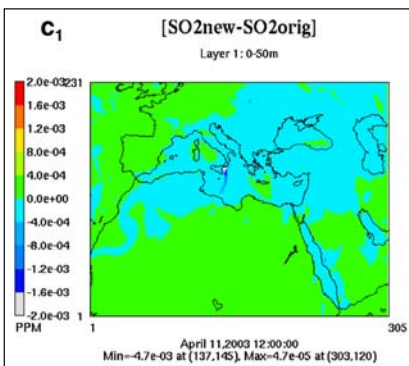
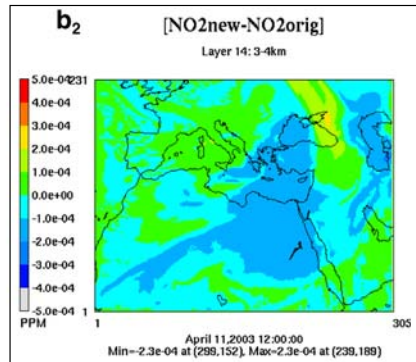
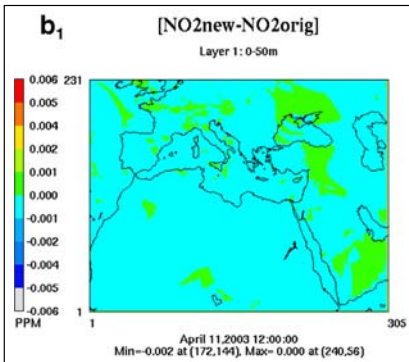
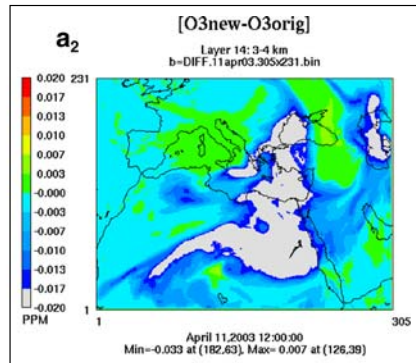
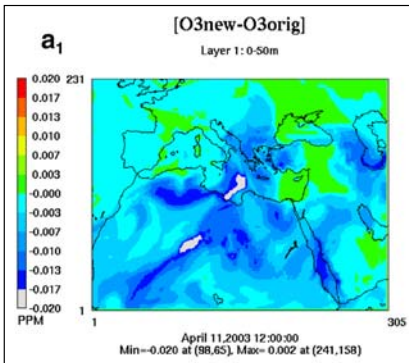
One aspect of the new processes embedded in the chemical transport model has been the production of new aerosols from the interaction of gases with aerosol surfaces. Another aspect is the impacts that these processes have on other species like ozone, sulfur dioxide and nitrogen oxides. In the previous section, the discussion focused on the ozone and sulfate reduction due to the shading effects of dust, for a small simulation period. The inclusion of all the gas-aerosol interaction processes changed the scenery by reducing ozone concentration up to 10–20 ppb at the surface and the upper layers of the model.

For ozone particularly, such reduction was useful and necessary when compared with observations in three locations in the Mediterranean region. During the case of April 2003, there were days with significant dust transport to the Eastern Mediterranean affecting Greece (10–15 April) and to the Western Mediterranean affecting Spain (14–18 April). For these days, the modeled ozone concentrations using the original version of CAMx and the version with the new processes compared to observations, revealed an improvement in the model performance (Fig. 6).

In Fig. 6, the blue line denotes the observed values, the green line is for the ozone concentration using the original version of the model and the red line is for the model with the new processes included. The ozone concentration simulated by the new model showed a decrease that enhanced the correlation with the observations. Model performance is different for each station due to their location. The station in Athens (Galatsi, Fig. 6a) is characterized as urban-background, whereas the two stations in Spain (Els Torms, Cabo de Creus, Fig. 6b, c) are characterized as rural background. Given the coarse horizontal resolution of the model, it is obvious that urban air quality cannot be resolved adequately, whereas for rural stations the model displays an overall substantial performance. For all the measuring sites, the trend line in the scatter diagrams showed enhanced performance when applying the new model development that lowered ozone concentration compared to the original code. Correlation coefficients also revealed an increase that reached 0.88 as shown in Fig. 6.

Besides the direct uptake of ozone on the dust particle (reaction 4, Sect. 2), the other gaseous species participating in the heterogeneous reactions influence the final ozone concentrations. The relative role of nitrogen oxide and nitric acid in the decrease of ozone concentrations is complicated and was the subject of several studies in the past (e.g. 29, 42, 44, 46 and 47). Overall, the mentioned decrease in ozone concentration is the result primarily of the heterogeneous processes and secondarily of the radiative effects of dust particles on photochemical processes as discussed in the sensitivity tests (Sect. 4.1).

Finally, the impacts of the interactions between gas-aerosol chemistry, on other species in the atmosphere are highlighted in Fig. 7 for April 11, 2003, at 12:00UTC. The differences shown in Fig. 7 are the result of two simulations with the chemical transport model, one with the original version of the code (named after 'orig') and one after implementing all the discussed processes (named after 'new'). Ozone concentration decrease appears in areas with high dust loading, as discussed previously. Ozone decrease reaches 20 ppb near the surface and 30 ppb at the upper model layer because of the new gas-aerosol interaction processes (Fig. 7a). Nitrogen dioxide is slightly decreased (maximum decrease 6 ppb) at the first layer and shows descending decrease at the higher layers (Fig. 7b). Likewise, sulfur dioxide is slightly decreased (maximum decrease 5 ppb, Fig. 7c), whereas nitric acid changes are more



◀ **Fig. 7** Changes in 2h average concentration in two vertical layers, 0–50 m (left graphs) and 3–4 km (right graphs) for: **(a)** Ozone, **(b)** Nitrogen dioxide, **(c)** Sulfur Dioxide and **(d)** Nitric Acid, for April 11, 2003, at 12:00UTC. The differences are the result of two simulations, one with the new processes and one with the original version of CAMx model

rapid and reach 20 ppb in the lowest model layer. The enhancement shown in all species in the upper layer can be attributed to the accumulated effects of low photolytic losses.

5 Summary and conclusions

The work presented in this paper has emphasized on the impacts of gas-aerosol chemistry interactions from the modeling point of view, focusing on the Euro-Mediterranean region.

Gases interact with aerosols like desert dust and sea-salt in various ways, including the direct radiative effects of particles on photochemical processes and the heterogeneous uptake of gases on dust particles that are discussed in the present study. The above interactions revealed that ozone anti-correlates with Saharan dust as has been stated in previous studies. The model performance concerning the ozone cycle has shown improvement according to statistics.

Sea-salt production embedded in the model has provided emissions of chloride and sodium species and an additional contribution to the particulate sulfate concentration. Sea-salt interacts with gases on an indirect way, enriching the chemical processes with the mentioned species that influence the cycle of other atmospheric pollutants.

The production of 3rd generation pollutants like particulate sulfates on dust particles seems to be important in areas with continuous and fresh release of sulfur dioxide together with the coexistence of dust particles, and of minor importance in other areas.

Third generation nitrates formed from the uptake of nitric dioxide on dust have shown negligible amounts compared to the anthropogenic nitrates, in agreement with the literature. Nitrates formed from the uptake of nitric acid were much higher in quantity and this result together with the model overestimation of the nitrates intensified the uncertainty of the constant uptake coefficient used for the relevant heterogeneous reaction.

The new model development discussed in the previous sections revealed the necessity of specified pollutant measurements including chemical speciation for the Mediterranean region. Also revealed the uncertainty of such processes based on the assumptions during the implementation of the relevant coefficients and algorithms. The generation of new aerosols and the removal of gases on dust surfaces can be significant for both the middle and the upper troposphere, not because of the high amounts of produced species, but due to the different properties of such generation. Interactions between gases and particles influence the atmospheric and chemical cycle of several other species, beyond the interacting ones. Combining this information with the capability of each species to affect solar radiation (absorption, scatter, extinction) and taking into account their deposition pathways, interesting insights can emerge on the potential climatic and environmental impacts for the Euro-Mediterranean region. Moreover, dust particles acting as reactive surfaces in a wet environment might lead to new climate modifiers for “desert dust-sensitive areas” like the Mediterranean region.

Acknowledgements This work is realized in the framework of Act.8.3 of the Operational Program Competitiveness (3rd Community Support Program) and is co-funded by 75% from the European Social Fund (EU), 25% from the Greek General Secretariat for Research and Technology (GSRT) under the project PENED 2003. The authors would like to acknowledge the contribution from Professor N. Mihalopoulos (ECPL, Department of Chemistry, Crete, Greece) and Dr. X. Querol (Institute of Earth Sciences, CSIC Barcelona) for providing

air quality measurements available at the framework of CIRCE project. We would also like to thank Professor Gregory Carmichael for his help and comments on the procedure used for the heterogeneous chemical reactions as well as the anonymous reviewers for their constructive comments and suggestions on the manuscript.

References

- Forster P, CoAuthors (2007) Changes in atmospheric constituents and in radiative forcing. In: Climate change 2007: the physical science basis. Contribution of working group I to the 4th IPCC assessment report. Cambridge University Press, Cambridge, United Kingdom and New York, NY, USA
- Kallos G, Kotroni V, Lagouvardos K, Papadopoulos A (1998) On the long-range transport of air pollutants from Europe to Africa. *Geophys Res Lett* 25:619–622. doi:[10.1029/97GL03317](https://doi.org/10.1029/97GL03317)
- Kallos G, Astitha M, Gofa F, O'Connor M, Mihalopoulos N, Zlatev Z (2004) Transport and deposition patterns of ozone and aerosols in the Mediterranean region. In: 27th NATO/CCMS international technical meeting on air pollution modeling and its applications, Banff, Canada, pp 218–225
- Kallos G, Papadopoulos A, Katsafados P, Nickovic S (2006) Trans-atlantic saharan dust transport: model simulation and results. *J Geophys Res*. doi:[10.1029/2005JD006207](https://doi.org/10.1029/2005JD006207)
- Kallos G, Astitha M, Katsafados P, Spyrou C (2007) Long-range transport of anthropogenically and naturally produced particulate matter in the Mediterranean and North Atlantic: current state of knowledge. *J Appl Meteorol Climatol* 46:1230–1251. doi:[10.1175/JAM2530.1](https://doi.org/10.1175/JAM2530.1)
- Rodríguez S, Querol X, Alastuey A, Kallos G, Kakaliagou O (2001) Saharan dust inputs to suspended particles time series (PM10 and TSP) in Southern and Eastern Spain. *Atmos Environ* 35:2433–2447. doi:[10.1016/S1352-2310\(00\)00496-9](https://doi.org/10.1016/S1352-2310(00)00496-9)
- Di Sarra A, Di Iorio T, Cacciani M, Fiocco G, Fuà D (2001) Saharan dust profiles measured by lidar from Lampedusa. *J Geophys Res* 106:10335–10347. doi:[10.1029/2000JD900734](https://doi.org/10.1029/2000JD900734)
- Kouvarakis G, Mihalopoulos N (2002) Seasonal variation of dimethylsulfide in the gas phase and of methanesulfonate and non-sea-salt sulfate in the aerosol phase measured in the Eastern Mediterranean atmosphere. *Atmos Environ* 36:929–938. doi:[10.1016/S1352-2310\(01\)00511-8](https://doi.org/10.1016/S1352-2310(01)00511-8)
- Viana MM, Querol X, Alastuey A, Cuevas E, Rodríguez S (2002) Influence of African dust on the levels of atmospheric particulates in the Canary Islands air quality network. *Atmos Environ* 36:5861–5875. doi:[10.1016/S1352-2310\(02\)00463-6](https://doi.org/10.1016/S1352-2310(02)00463-6)
- Sciare J, Bardouki H, Moulin C, Mihalopoulos N (2003) Aerosol sources and their contribution to the chemical composition of aerosols in the Eastern Mediterranean Sea during summertime. *Atmos Chem Phys* 3:291–302
- Querol X, Alastuey A, Ruiz CR, Artiñano B, Hansson HC, Harrison RM, Buringh E, ten Brink HM, Lutz M, Bruckmann P, Straehl P, Schneider J (2004a) Speciation and origin of PM10 and PM2.5 in selected European cities. *Atmos Environ* 6547–6555. doi:[10.1016/j.atmosenv.2004.08.037](https://doi.org/10.1016/j.atmosenv.2004.08.037)
- Querol X, Alastuey A, Viana MM, Rodríguez S, Artiñano B, Salvador P, Garcia dos Santos S, Fernandez Patier R, Ruiz CR, de la Rosa J, Sanchez de la Campa A, Menendez M, Gil JI (2004b) Speciation and origin of PM10 and PM2.5 in Spain. *J Aerosol Sci* 35:1151–1172. doi:[10.1016/j.jaerosci.2004.04.002](https://doi.org/10.1016/j.jaerosci.2004.04.002)
- Astitha M, Kallos G, Katsafados P, Pytharoulis I, Mihalopoulos N (2006) Radiative effects of natural PMs on photochemical processes in the Mediterranean region. In: Borrego C, Renner E (eds) 28th NATO/CCMS ITM, May 2006, Leipzig, Germany, Oral presentation-proceedings, Elsevier pub., pp 548–559, ISBN: 978-0-444-52987-9
- Astitha M, Kallos G, Katsafados P, Mavromatidis E (2007) Heterogeneous chemical processes and their role on particulate matter formation in the Mediterranean region. In: 29th NATO/CCMS ITM, September 2007, Aveiro, Portugal
- Alastuey A, CoAuthors (2005) Characterisation of TSP and PM2.5 at Izana and Sta Cruz de Tenerife (Canary Islands, Spain) during a Saharan dust episode. *Atmos Environ* 39:4715–4728. doi:[10.1016/j.atmosenv.2005.04.018](https://doi.org/10.1016/j.atmosenv.2005.04.018)
- Fountoukis C, Nenes A (2007) ISORROPIA II: a computationally efficient thermodynamic equilibrium model for K^+ – Ca^{2+} – Mg^{2+} – NH_4^+ – Na^+ – SO_4^{2-} – NO_3^- – Cl^- – H_2O aerosols. *Atmos Chem Phys Discuss* 7:1893–1939
- Ramanathan V, Crutzen PJ, Kiehl JT, Rosenfeld D (2001) Aerosols, climate and the hydrologic cycle. *Science* 294:2119–2124. doi:[10.1126/science.1064034](https://doi.org/10.1126/science.1064034)
- Levin Z, Teller A, Ganor E, Yin Y (2005) On the interactions of mineral dust, sea-salt particles and clouds: a measurement and modelling study from the Mediterranean Israeli Dust Experiment campaign. *J Geophys Res*. doi:[10.1029/2005JD005810](https://doi.org/10.1029/2005JD005810)
- Rosenfeld D (2006) Aerosols, clouds and climate. *Science* 312:1323–1324. doi:[10.1126/science.1128972](https://doi.org/10.1126/science.1128972)

20. Shankar U, Bhawe PV, Vukovich JM, Roselle SJ (2005) Implementation and initial applications of sea salt aerosol emissions and chemistry algorithms in the CMAQ v4.5-AERO4 module. In: 4th annual CMAS models-3 users' conference
21. Gong SL, Barrie LA, Blanchet JP (1997) Modeling sea-salt aerosols in the atmosphere 1. Model development. *J Geophys Res* 102:3805–3818. doi:[10.1029/96JD02953](https://doi.org/10.1029/96JD02953)
22. Gong SL (2003) A parameterization of sea-salt aerosol source function for sub- and super-micron particles. *Glob Biogeochem Cycles*. doi:[10.2929/2003GB002079](https://doi.org/10.2929/2003GB002079)
23. Environ (2006) User's guide to the Comprehensive Air Quality Model with Extensions (CAMx). Version 4.31. Prepared by ENVIRON Inter. Corp., Novato, CA
24. Zhang KM, Knipping EM, Wexler AS, Bhawe PV, Tonnesen GS (2005) Size distribution of sea-salt emissions as a function of relative humidity. *Atmos Environ* 39:3373–3379. doi:[10.1016/j.atmosenv.2005.02.032](https://doi.org/10.1016/j.atmosenv.2005.02.032)
25. de Leeuw G, Neele FP, Hill M, Smith MH, Vignati E (2000) Production of sea spray aerosol in the surf zone. *J Geophys Res* 105(D24):29397–29409. doi:[10.1029/2000JD900549](https://doi.org/10.1029/2000JD900549)
26. Gong SL, Barrie LA, Lazare M (2002) Canadian Aerosol Module (CAM): a size-segregated simulation of atmospheric aerosol processes for climate and air quality models: 2. Global sea-salt aerosol and its budgets. *J Geophys Res* 107(D24):4779. doi:[10.1029/2001JD002004](https://doi.org/10.1029/2001JD002004)
27. Fuchs NA, Sutugin AG (1970) Highly dispersed aerosols. Ann Arbor Science Publishers, Ann Arbor, MI
28. Saylor RD (1997) An estimate of the potential significance of heterogeneous loss to aerosols as an additional sink for HO radicals in the troposphere. *Atmos Environ* 21:3653–3658. doi:[10.1016/S1352-2310\(97\)00143-X](https://doi.org/10.1016/S1352-2310(97)00143-X)
29. Dentener FJ, Carmichael GR, Zhang Y, Lelieveld J, Crutzen PJ (1996) The role of mineral aerosols as a reactive surface in the global troposphere. *J Geophys Res* 101:22869–22889. doi:[10.1029/96JD01818](https://doi.org/10.1029/96JD01818)
30. Seisel S, Keil T, Lian Y, Zellner R (2006) Kinetics of the uptake of SO₂ on mineral oxides: improved initial uptake coefficients at 298 K from pulsed Knudsen cell experiments. *Int J Chem Kinet* 38:242. doi:[10.1002/kin.20148](https://doi.org/10.1002/kin.20148)
31. Chang RY-W, Sullivan RC, Abbatt JPD (2005) Initial uptake of ozone on Saharan dust at atmospheric relative humidities. *Geophys Res Lett*. doi:[10.1029/2005GL023317](https://doi.org/10.1029/2005GL023317)
32. Adams JW, Rodriguez D, Cox RA (2005) The uptake of SO₂ on Saharan dust: a flow tube study. *Atmos Chem Phys* 5:2679–2689
33. Seisel S, Borensen C, Vogt R, Zellner R (2004) The heterogeneous reaction of HNO₃ on mineral dust and gamma-alumina surfaces: a combined Knudsen cell and DRIFTS study. *Phys Chem Chem Phys* 6:5498–5508. doi:[10.1039/b410793d](https://doi.org/10.1039/b410793d)
34. Ullerstam M, Johnson MS, Vogt R, Ljungstrom E (2003) DRIFTS and Knudsen cell study of the heterogeneous reactivity of SO₂ and NO₂ on mineral dust. *Atmos Chem Phys* 3:2043–2051
35. Hanisch F, Crowley JN (2003) Heterogeneous reactivity of NO and HNO₃ on mineral dust in the presence of ozone. *Phys Chem Chem Phys* 883–887. doi:[10.1039/b211503d](https://doi.org/10.1039/b211503d)
36. Usher CR, Al-Hosney H, Carlos-Cuellar S, Grassian VH (2002) A laboratory study of the heterogeneous uptake and oxidation of sulfur dioxide on mineral dust particles. *J Geophys Res A*. doi:[10.1029/2002JD002051](https://doi.org/10.1029/2002JD002051)
37. Ullerstam M, Vogt R, Langer S, Ljungstrom E (2002) The kinetics and mechanism of SO₂ oxidation by O₃ on mineral dust. *Phys Chem Chem Phys* 4:4694–4699. doi:[10.1039/b203529b](https://doi.org/10.1039/b203529b)
38. Hanisch F, Crowley JN (2001) Heterogeneous reactivity of gaseous nitric acid on Al₂O₃, CaCO₃, and atmospheric dust samples: a Knudsen cell study. *J Phys Chem* 105:3096–3106
39. Underwood GM, Song CH, Phadnis M, Carmichael GR, Grassian VH (2001) Heterogeneous reactions of NO₂ and HNO₃ on oxides and mineral dust: a combined laboratory and modeling study. *J Geophys Res* 106:18055–18066. doi:[10.1029/2000JD900552](https://doi.org/10.1029/2000JD900552)
40. Goodman AL, Li P, Usher CR, Grassian VH (2001) Heterogeneous uptake of sulfur dioxide on aluminum and magnesium oxide particles. *J Phys Chem A* 105:6109–6120. doi:[10.1021/jp004423z](https://doi.org/10.1021/jp004423z)
41. Bauer SE, Koch D (2005) Impact of heterogeneous sulfate formation at mineral dust surfaces on aerosol loads and radiative forcing in the Goddard Institute for Space Studies general circulation model. *J Geophys Res* 110(D17). doi:[10.1029/2005JD005870](https://doi.org/10.1029/2005JD005870)
42. Tang Y, Carmichael GR, Kurata G, Uno I, Weber RJ, Song C, Guttikunda SK, Woo JH, Streets DG, Wei C, Clarke AD, Huebert B, Anderson TL (2004) Impacts of dust on regional tropospheric chemistry during the ACE-Asia experiment: a model study with observations. *J Geophys Res*. doi:[10.1029/2003JD003806](https://doi.org/10.1029/2003JD003806)
43. Liao H, Seinfeld JH, Adams PJ, Mickley LJ (2004) Global radiative forcing of tropospheric ozone and aerosols in a unified general circulation model. *J Geophys Res* 109(D16207). doi:[10.1029/2003JD004456](https://doi.org/10.1029/2003JD004456)

44. Bauer SE, Balkanski Y, Schulz M, Hauglustaine DA, Dentener F (2004) Global modeling of heterogeneous chemistry on mineral aerosol surfaces: influence on tropospheric ozone chemistry and comparison to observations. *J Geophys Res Atmos*. doi:[10.1029/2003JD003868](https://doi.org/10.1029/2003JD003868)
45. Liao H, Adams PJ, Chung SH, Seinfeld JH, Mickley LJ, Jacob D (2003) Interactions between tropospheric chemistry and aerosols in a unified general circulation model. *J Geophys Res*. doi:[10.1029/2001JD001260](https://doi.org/10.1029/2001JD001260)
46. Bian H, Zender CS (2003) Mineral dust and global tropospheric chemistry: relative role of photolysis and heterogeneous uptake. *J Geophys Res*. doi:[10.1029/2002JD003143](https://doi.org/10.1029/2002JD003143)
47. Zhang Y, Carmichael GR (1999) The role of mineral aerosol in tropospheric chemistry in East Asia-A model study. *J Appl Meteorol* 38:353–366. doi:[10.1175/1520-0450\(1999\)038<0353:TROMAI>2.0.CO;2](https://doi.org/10.1175/1520-0450(1999)038<0353:TROMAI>2.0.CO;2)
48. Kallos G (1997) The regional weather forecasting system SKIRON: an overview. In: Proceedings of the symposium on regional weather prediction on parallel computer environments. University of Athens, Greece, pp 109–122
49. Nickovic S, Kallos G, Papadopoulos A, Kakaliagou O (2001) A model for prediction of desert dust cycle in the atmosphere. *J Geophys Res* 106(D16):18113–18129. doi:[10.1029/2000JD900794](https://doi.org/10.1029/2000JD900794)
50. Tegen I, Fung I (1994) Modelling of mineral dust in the atmosphere: sources, transport and optical thickness. *J Geophys Res* 99:22897–22914. doi:[10.1029/94JD01928](https://doi.org/10.1029/94JD01928)
51. Nenes A, Pilinis C, Pandis SN (1998) ISORROPIA: a new thermodynamic model for multiphase multicomponent inorganic aerosols. *Aquat Geochem* 4:123–152. doi:[10.1023/A:1009604003981](https://doi.org/10.1023/A:1009604003981)
52. Seinfeld J, Pandis S (1998) Atmospheric chemistry and physics (From air pollution to climate change). John Wiley and Sons, Inc.
53. Tegen I, Hollrig P, Chin M, Fung I, Jacob D, Penner JE (1997) Contribution of different aerosol species to the global aerosol extinction optical thickness: estimates from model results. *J Geophys Res Atmos* 102:23895–23915. doi:[10.1029/97JD01864](https://doi.org/10.1029/97JD01864)
54. Chin M, Ginoux P, Kinne S, Torres O, Holben BN, Duncan BN, Martin RV, Logan JA, Higurashi A, Nakajima T (2002) Tropospheric aerosol optical thickness from the GOCART model and comparisons with satellite and sun photometer measurements. *J Atmos Sci* 59:461–483. doi:[10.1175/1520-0469\(2002\)059<0461:TAOTFT>2.0.CO;2](https://doi.org/10.1175/1520-0469(2002)059<0461:TAOTFT>2.0.CO;2)
55. Anderson JL, Coauthors (2004) The new GFDL global atmosphere and land model AM2–LM2: evaluation with prescribed SST simulations. *J Clim* 17(24):4641–4673. doi:[10.1175/JCLI-3223.1](https://doi.org/10.1175/JCLI-3223.1)
56. Madronich S (2002) The Tropospheric Visible Ultraviolet (TUV) model web page. National Center for Atmospheric Research: Boulder, CO, 2002. <http://www.acd.ucar.edu/TUV/>
57. Madronich S (1993) UV radiation in the natural and perturbed atmosphere. In: Tevini M (ed) Environmental effects of UV (Ultraviolet) radiation. Lewis: Boca Raton, FL, pp 17–69
58. Chang JS, Brost RA, Isaksen ISA, Madronich S, Middleton P, Stockwell WR, Walcek CJ (1987) A three-dimensional Eulerian Acid Deposition Model: Physical concepts and formulation. *J Geophys Res* 92:14681–14700. doi:[10.1029/JD092iD12p14681](https://doi.org/10.1029/JD092iD12p14681)
59. Elterman L (1968) UV, visible and IR attenuation for altitudes to 50 km. AFCRL-68-0153, 49 pp; Air Force Cambridge Res. Labs., Hanscom AFB, Mass
60. Balis DS, Zerefos CS, Kourtidis K, Bais F, Hofzumahaus A, Kraus R, Schmitt M, Gobbi GP (2002) Measurements and modeling of photolysis rates during the Photochemical Activity and Ultraviolet Radiation (PAUR) II campaign. *J Geophys Res*. doi:[10.1029/2000DJ000136](https://doi.org/10.1029/2000DJ000136)
61. Gerasopoulos E, Kouvarakis G, Vrekoussis M, Donoussis C, Mihalopoulos N, Kanakidou M (2006) Photochemical ozone production in the Eastern Mediterranean. *Atmos Environ* 40:3057–3069. doi:[10.1016/j.atmosenv.2005.12.061](https://doi.org/10.1016/j.atmosenv.2005.12.061)
62. Martin VM, Jacob DJ, Yantosca RM, Chin M, Ginoux P (2003) Global and regional decreases in tropospheric oxidants from photochemical effects of aerosols. *J Geophys Res* 108(D3):4097. doi:[10.1029/2002JD002622](https://doi.org/10.1029/2002JD002622)
63. Bardouki H, Liakakou H, Economou C, Smolic J, Zdimal V, Eleftheriadis K, Lazaridis M, Mihalopoulos N (2003) Chemical composition of size resolved atmospheric aerosols in the Eastern Mediterranean during summer and winter. *Atmos Environ* 37:195–208. doi:[10.1016/S1352-2310\(02\)00859-2](https://doi.org/10.1016/S1352-2310(02)00859-2)
64. Seigneur C, Pun B, Chen SY, Lohman K (2004) Performance evaluation of four air quality models applied for an annual simulation of PM over the Western United States. Final Report, CRC Project-A44
65. Hertel O, Ambelas Skjøth C, Frohn LM, Vignati E, Frydendall J, de Leeuw G, Schwarz U, Reis S (2002) Assessment of the atmospheric nitrogen and sulphur inputs into the North Sea using a Lagrangian Model. *Phys Chem Earth* 27:1507–1515